

Quantum reflection from an atomic mirror

B. Segev and R. Côté

*Institute for Theoretical Atomic and Molecular Physics (ITAMP),
Harvard-Smithsonian Center for Astrophysics, 60 Garden Street, Cambridge, Massachusetts 02138*

M. G. Raizen

Department of Physics, The University of Texas at Austin, Austin, Texas 78712-1081

(Received 31 July 1997)

We calculate the reflection probability for ultracold atoms incident on an evanescent-wave atomic mirror, and analyze the optimum conditions to observe quantum reflection. We find that averaging over the Gaussian profile of the laser beam dramatically reduces the quantum signature, and consider the effects of an appropriate aperture that limits the variation of beam intensity. We show that quantum reflection is particularly sensitive to details of the atom-surface potential, and could be used to resolve retardation effects.

[S1050-2947(97)50611-1]

PACS number(s): 42.50.Vk, 34.20.-b

Recent experimental developments enable precise manipulation of cold atoms by lasers [1,2]. Small and accurate velocities of the atoms can be achieved using advanced cooling [3–5] and launching [6,7] techniques, and a detuned laser field can be used to create controlled and adjustable potentials for the atoms [2,8]. Under these conditions, the quantum nature of the dynamics may become important [9,10]. Indeed, quantum tunneling of atoms has recently been observed [11,12], and in this Rapid Communication we analyze the conditions to observe quantum reflection, i.e., above-barrier, classically forbidden reflection of atoms from evanescent-wave mirrors [10].

Reflection from such an atomic mirror was recently used to measure the van der Waals force between a dielectric surface and an atom in its ground state [13]. In this landmark experiment, cold ^{85}Rb atoms with a kinetic energy $E \approx 4.75 \times 10^{-9}$ a.u. (atomic units) corresponding to a velocity of 54 cm/s were used. The reflection was of a classical nature; to a good approximation *only* atoms with under-barrier energies $E < V_{\text{max}}$ were reflected, where V_{max} is the maximum height of the barrier. We consider here a similar experiment in the quantum regime. For colder atoms, in an energy range of $E \approx 5 \times 10^{-11}$ a.u., the reflection probability curves would differ from the classical Heaviside function. Unlike classical reflection, which can only be used to identify thresholds and to measure V_{max} , quantum probabilities are determined by the complete potential curve, and are particularly sensitive to the short- and long-range behavior of the potential. The sensitivity of over-barrier reflection to details of the potential may be used in the future to further study the atom-surface interaction.

An evanescent-wave atomic mirror is obtained when blue-detuned light undergoes total internal reflection inside a dielectric prism. The induced dipole interaction with the evanescent light field outside the surface of the prism creates an effective repulsive optical potential for the incident atoms [2,14–16]. This potential is proportional to the intensity of the laser I , to the square of the atomic dipole moment d , and inversely proportional to the detuning Δ . The strength of the repulsive potential at the surface of the prism can be adjusted by changing the intensity of the laser while keeping the de-

tuning large enough so as to minimize spontaneous emission. On the surface of the prism, the repulsive potential decreases slowly due to the Gaussian profile of the laser beam. In the direction perpendicular to the prism surface, the potential exhibits a fast exponential decline due to the exponentially decreasing intensity of the evanescent wave. Thus, the evanescent-wave potential is $C_0 \exp(-\rho^2) \exp(-2\kappa z)$, where $C_0 \propto Id^2/\Delta$ is the maximum value of the repulsive potential, ρ is a dimensionless parameter for the transverse distance from the center of the Gaussian beam, and $\kappa = k \sqrt{n^2 \sin^2 \theta - 1}$, where k is the wave number of the laser light, θ is the incident angle of the light with the normal to the surface of the prism, and n is the index of refraction.

Atoms incident on the evanescent-wave atomic mirror move in an effective potential that is a combination of the light-induced repulsive potential and an attractive atom-wall interaction. The interaction between a ground-state atom and a dielectric or conducting wall has been investigated theoretically [17–22] and experimentally [13,23–25]. Theoretical studies have been performed on different levels, from a simple model of a dipole-dipole interaction of the atom and its mirror image, to the full QED relativistic quantum treatment. Interesting in particular are the long-range Casimir interactions [22] that were recently observed in cavity QED experiments [24,25]. The detailed interaction between a ground-state sodium atom and a perfectly conducting wall including the long-range retardation effects was recently calculated [26]. Although the interaction potential of a sodium atom with a dielectric surface is not yet available, the Lennard-Jones coefficient can be scaled with the index of refraction in a simple way. The attractive atom-wall potential in this approximation is $-C_3^{(n)}/z^3$, where $C_3^{(n)} = (n^2 - 1)/(n^2 + 1) C_3^{\text{metal}}$ and $C_3^{\text{metal}} = 1.5753$ a.u. for sodium [26].

The combined physical potential is, therefore,

$$V(\rho, z) = C_0 \exp(-\rho^2) \exp(-2\kappa z) - \frac{C_3^{(n)}}{z^3}. \quad (1)$$

The interaction potential of Eq. (1) for a ground-state Na atom is shown in Fig. 1(a). The maximum value of the po-

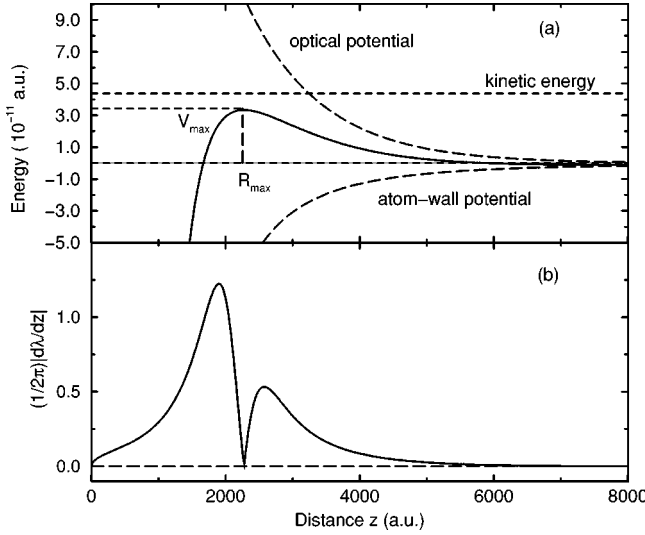


FIG. 1. The interaction potential (a) is formed by an optical potential due to total internal reflection in a prism, and the atom-wall purely attractive potential. The classical threshold value $C_0 = \Gamma$ is found by adjusting C_0 so that the maximum of the potential V_{\max} would be equal to the kinetic energy E . In (b) we show the “badlands” associated with (a). We notice two regions corresponding to the fast inner power-law drop, and the long-range exponential tail. These curves are for $n = 1.805$ and $\theta = 45^\circ$, i.e., $C_3 = 0.8354$ a.u., and $\kappa = 4.4771 \times 10^{-4}$ a.u. with $\Gamma = 8.7623 \times 10^{-10}$ a.u. We selected Na atoms with $v = 10$ cm/s (or $E = 4.378 \times 10^{-11}$ a.u.) and $C_0 = 8.0 \times 10^{-10}$ a.u. (here $\rho = 0$).

tential V_{\max} can be adjusted by changing C_0 , which in Fig. 1(a) was chosen to be an order of magnitude smaller than in Ref. [13]. The width of the potential and its slopes are sensitive to the physical details. The index of refraction of the prism, for example, affects both κ , the slope of the exponential decline of the dipole interaction with the evanescent wave, and $C_3^{(n)}$, the amplitude of the attractive atom-wall potential. Some potential curves for different choices of n and θ are plotted in Fig. 2(a).

The reflection probability $|R|^2$, as a function of the energy of the atoms and of the intensity of the laser, was evaluated by numerically integrating the Schrödinger equation for different values of E and C_0 in the method of Ref. [27]. Quantum effects, such as over-barrier reflection and under-barrier transmission, are dominated by regions of the potential where the semiclassical treatment fails [27]. In the case of the atomic mirror potential of Figs. 1(a), 2(a), and Eq. (1), the de Broglie wavelength varies slowly in the limits $z \rightarrow \infty$ and $z \rightarrow 0$, where

$$\frac{1}{2\pi} \left| \frac{d\lambda}{dz} \right| = \hbar \left| \frac{m}{p^3} \frac{dV}{dz} \right| \ll 1,$$

but there are “badlands” in between, where the Wentzel-Kramers-Brillouin (WKB) approximation breaks down. In Fig. 1(b) two such “badlands” are shown for the potential of Fig. 1(a): a smaller one due to the long-range tail of the potential and a stronger one caused by the inner portion of the potential. The quantum reflection probability curves for the potentials of Fig. 2(a), are plotted, for example, in Fig. 2(b). The numerical simulations indicate that the sharp

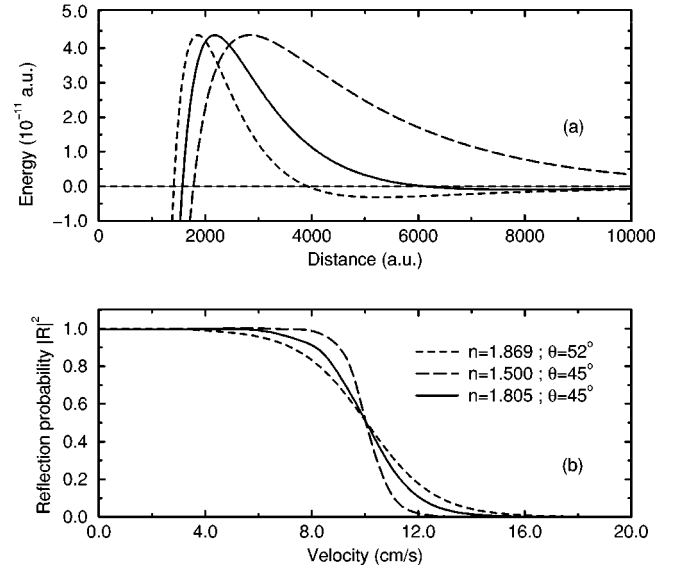


FIG. 2. Three different potentials for Na, corresponding to different sets of n and θ (different prisms), are shown in (a). All have the same V_{\max} set at 4.378×10^{-11} a.u. (10 cm/s), and thus the same threshold for classical reflection. In (b) the corresponding quantum reflection probabilities $|R|^2$ are shown as a function of the velocity v .

power-law decline in the inner side of the potential substantially increases the quantum over-barrier reflection.

In one dimension, classical reflection is characterized by the Heaviside step function, while quantum reflection can be recognized by its S-shaped curves. In an actual experiment, the Gaussian profile of the laser beam has to be taken into account. The signature for classical reflection is then a logarithmic dependence of the integrated reflection signal on the intensity of the laser [13]. Quantum behavior would still be characterized by S-shaped probability curves, but averaging over the Gaussian profile will obscure the difference between classical and quantum behavior. In order to reduce the averaging effect, and at the same time calibrate the incident and reflected fluxes, we suggest limiting the size of the mirror, using a circular aperture so as to have $0 \leq \rho \leq r$.

An experiment could be performed in the following way. A uniform flux of atoms with an average velocity of 10 cm/s would be created and launched on a finite-size atomic mirror with the potential profile of Eq. (1) with $n = 1.869$, $\theta = 52^\circ$, and $k = 5.645 \times 10^{-4}$ a.u. or $\lambda = 589$ nm. Changing C_0 , starting from zero (pure attractive potential) and gradually increasing the intensity of the laser beam, one increases the reflection signal, until a plateau of total reflection is reached. In classical mechanics the reflected signal is proportional to the area of that part of the mirror where $V_{\max} > E$, which gives a linear behavior of the integrated reflection probabilities as a function of $\ln C_0$. Normalizing the reflection signal at the plateau to 1, the slope of the logarithmic curve for classical reflection from the finite-size atomic mirror is inversely proportional to the area of the mirror. The critical value of $C_0 = \Gamma$, which gives the threshold for classical reflection, is obtained from solving $V_{\max} = E$. The properties of the classical reflection reference curves are given in Fig. 3. The quantum S-shaped curves are obtained from numerically solving the Schrödinger equation and integrating over ρ up to r .

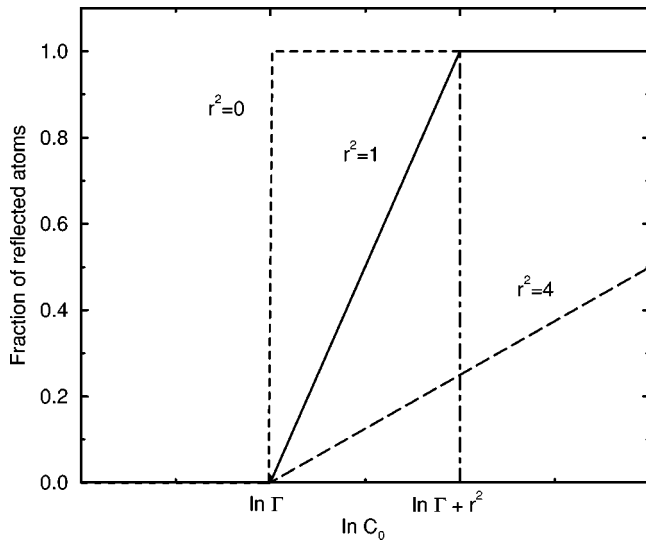


FIG. 3. Classical reference curves for the fraction of reflected atoms, averaged over the Gaussian profile of the beam up to the radius of the aperture, r . There is no classical reflection below the threshold value, i.e., for $C_0 \leq \Gamma$. The classical reflection is complete for $\ln C_0 \geq \ln \Gamma + r^2$. In between, the fraction of reflected atoms as a function of $\ln C_0$ exhibits a linear increase with a slope of $1/r^2$ (inversely proportional to the area of the aperture).

They are compared to the classical lines in Figs. 4 and 5 for different sizes of the mirror (i.e., different r) and for different incident velocities, respectively. Two quantum effects can be observed in the one-dimensional curves of Fig. 2(b). The reflection probabilities at energies above the barrier are larger than zero and the under-barrier reflection probabilities are smaller than 1, due to tunneling. A cancellation between these two effects is obtained when atoms are reflected from the three-dimensional potential due to the effective averaging over the Gaussian profile of the beam. Having a finite radius aperture is therefore essential in distinguishing quantum from classical behavior (see Fig. 4). For a small enough aperture, the quantum probabilities clearly deviate from the logarithmic behavior of classical reflection. In order to ob-

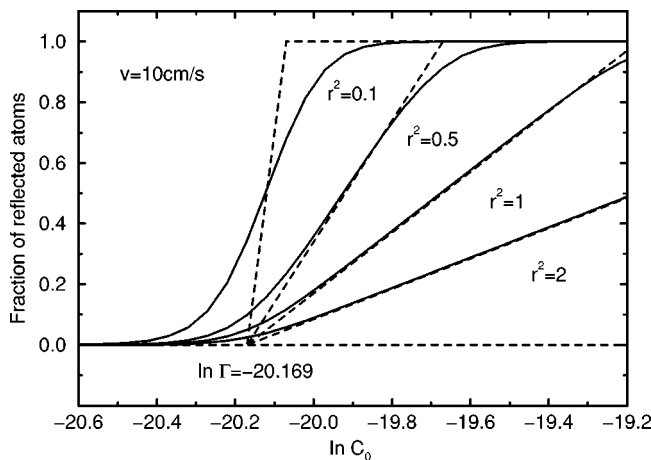


FIG. 4. Comparison of quantum (solid lines) and classical (dashed lines) reflection curves for different radii of the aperture r , as a function of $\ln C_0$ for Na at $v = 10$ cm/s ($n = 1.869$, $\theta = 52^\circ$, and $k = 5.645 \times 10^{-4}$ a.u. or $\lambda = 589$ nm). The classical threshold is at $\Gamma = 1.7398 \times 10^{-9}$ a.u.

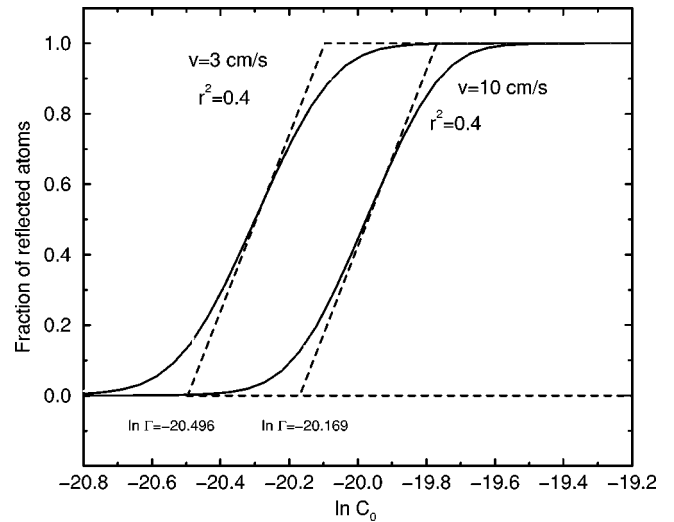


FIG. 5. Same as Fig. 4, with a given radius r , for Na at different velocities corresponding to different values for the classical threshold of C_0 . Shown here are $\Gamma = 1.2558 \times 10^{-9}$ a.u. for $v = 3$ cm/s and $\Gamma = 1.7398 \times 10^{-9}$ a.u. for $v = 10$ cm/s.

serve quantum behavior, the velocities of the atoms must be small enough so that the de Broglie wavelength is of the same order of magnitude as the badlands' width. The smaller the velocity, the larger the quantum signature, but, once in the quantum regime, the main effect of small changes in the velocity is to change Γ , the critical value of C_0 that gives the threshold for classical reflection (see Fig. 5).

The long-range (Casimir) interactions due to retardation may have an observable effect on the quantum reflection probabilities. The reflection probabilities from the purely attractive potential of sodium atoms in their ground state interacting with a conducting surface, with and without taking retardation into account, are shown in Fig. 6. The atom-wall potential curves were taken from Ref. [26]. The long-range interaction due to retardation substantially increases quantum reflection in this case, but the velocities needed to observe this effect are extremely small. This is to be expected since a

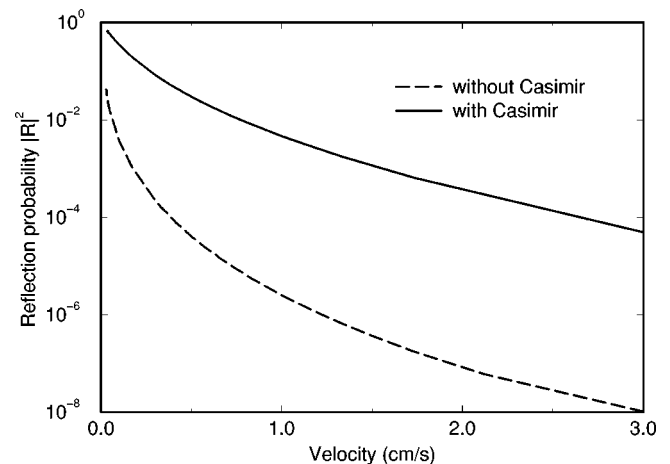


FIG. 6. Comparison of quantum reflection for purely attractive potentials, with (solid line) and without (dashed line) Casimir interactions, in the case of a conducting surface with Na atoms. The reflection probability $|R|^2$ is many orders of magnitude bigger with Casimir interactions than without.

change in the power law of the purely attractive potential modifies $|R|^2$ drastically at threshold [27]. More theoretical work is needed in order to include retardation in the potential curves and in the reflection probability calculations for sodium atoms incident on the dielectric prism.

In conclusion, we have shown that cold atoms incident on an evanescent-wave atomic mirror with sufficiently small velocities (e.g., 10 cm/s for sodium atoms) will exhibit quantum dynamics. Atoms with energies above the maximum of the potential barrier will undergo classically forbidden reflection. An S-shaped probability curve is predicted for the fraction of reflected atoms as a function of the logarithm of the laser intensity. In order to observe this S-shaped curve, which is typical of quantum behavior, the variation of intensity across the atomic mirror must be minimized. Unlike re-

flexion in the classical domain, quantum reflection depends on the details of the potential, both at short and large distances. This sensitivity and the ability to control the optical potential could be used in the future to probe the atom-wall interaction. Finally, we explored the consequences of retardation effects on the reflection probabilities.

We thank Dr. J. Babb for very useful discussions. R.C. and B.S. are supported by the National Science Foundation through a grant for the Institute for Theoretical Atomic and Molecular Physics at Harvard University and Smithsonian Astrophysical Observatory. The work of M.G.R. is supported by the R. A. Welch Foundation and the National Science Foundation.

-
- [1] S. Chu, *Science* **253**, 861 (1991).
 [2] C. S. Adams, M. Sigel, and J. Mlynek, *Phys. Rep.* **240**, 143 (1994).
 [3] M. Kasevich and S. Chu, *Phys. Rev. Lett.* **69**, 1741 (1992).
 [4] J. Lawall, F. Bardou, B. Saubamea, K. Shimizu, M. Leduc, A. Aspect, and C. Cohen-Tannoudji, *Phys. Rev. Lett.* **73**, 1915 (1994).
 [5] J. Reichel, F. Bardou, M. Ben-Dahan, E. Peik, S. Rand, C. Solomon, and C. Cohen-Tannoudji, *Phys. Rev. Lett.* **75**, 4575 (1995).
 [6] S. R. Wilkinson, C. F. Bharucha, K. W. Madison, Q. Niu, and M. G. Raizen, *Phys. Rev. Lett.* **76**, 4512 (1996).
 [7] M. Ben Dahan, E. Peik, J. Reichel, Y. Castin, and C. Salomon, *Phys. Rev. Lett.* **76**, 4508 (1996).
 [8] M. G. Prentiss, *Science* **260**, 1078 (1993).
 [9] F. L. Moore, J. C. Robinson, C. F. Bharucha, P. E. Williams, and M. G. Raizen, *Phys. Rev. Lett.* **73**, 2974 (1994).
 [10] C. Henkel, C. I. Westbrook, and A. Aspect, *J. Opt. Soc. Am. B* **13**, 233 (1996).
 [11] C. F. Bharucha, K. W. Madison, P. R. Morrow, S. R. Wilkinson, Bala Sundaram, and M. G. Raizen, *Phys. Rev. A* **55**, R857 (1997).
 [12] E. Peik, M. Ben-Dahan, I. Bouchoule, Y. Castin, and C. Salomon, *Phys. Rev. A* **55**, 2989 (1997).
 [13] A. Landragin, J. Y. Courtois, G. Labeyrie, N. Vansteenkiste, C. I. Westbrook, and A. Aspect, *Phys. Rev. Lett.* **77**, 1464 (1996).
 [14] R. J. Cook and R. K. Hill, *Opt. Commun.* **43**, 258 (1982).
 [15] V. I. Balykin, V. S. Letokhov, Y. B. Ovchinnikov, and A. I. Sidorov, *Pis'ma Zh. Eksp. Teor. Fiz.* **45**, 282 (1987) [*JETP Lett.* **45**, 353 (1987)].
 [16] M. A. Kasevich, D. S. Weiss, and S. Chu, *Opt. Lett.* **15**, 607 (1990).
 [17] L. E. Lennard-Jones, *Trans. Faraday Soc.* **28**, 333 (1932).
 [18] H. B. G. Casimir and D. Polder, *Phys. Rev.* **73**, 360 (1948).
 [19] I. E. Dzyaloshinskii, E. M. Lifshitz, and L. P. Pitaevskii, *Adv. Phys.* **10**, 165 (1961).
 [20] L. Spruch and Y. Tikochinsky, *Phys. Rev. A* **48**, 4213 (1993).
 [21] Y. Tikochinsky and L. Spruch, *Phys. Rev. A* **48**, 4223 (1993).
 [22] L. Spruch, *Science* **272**, 1452 (1996).
 [23] M. Kasevich, K. Moler, E. Riis, E. Sunderman, D. Weiss, and S. Chu, in *Atomic Physics 12*, edited by J. C. Zorn and R. R. Lewis, AIP Conf. Proc. No. 233 (AIP, New York, 1991), p. 47.
 [24] V. Sandoghdar, C. I. Sukenik, E. A. Hinds, and S. Haroche, *Phys. Rev. Lett.* **68**, 3432 (1992).
 [25] C. I. Sukenik, M. G. Boshier, D. Cho, V. Sandoghdar, and E. A. Hinds, *Phys. Rev. Lett.* **70**, 560 (1993).
 [26] M. Marinescu, A. Dalgarno, and J. F. Babb, *Phys. Rev. A* **55**, 1530 (1997).
 [27] R. Côté, H. Friedrich, and J. Trost, *Phys. Rev. A* **56**, 1781 (1997).